

Low-Temperature Growth of Single-Walled Carbon Nanotubes by Plasma Enhanced Chemical Vapor Deposition

Eun Ju Bae, Yo-Sep Min, Donghun Kang, Ju-Hye Ko, and Wanjun Park*

Materials and Devices Research Center, Samsung Advanced Institute of Technology, Yong-In, Kyeonggi-Do 449-712, Korea

Received April 27, 2005. Revised Manuscript Received July 26, 2005

Single-walled carbon nanotubes (SWNTs) were successfully grown on SiO₂/Si substrates at 450 °C by remote plasma enhanced chemical vapor deposition with a plasma power of 15 W. The ratio of D-band (disorder-induced mode) to G-band (tangential stretching mode) in the Raman spectra, an indicator of nanotube quality, is about 0.1 owing to their good quality. Even at 400 °C, SWNTs were also grown with low plasma power (<40 W), although the I_D/I_G ratios are higher than those at 450 °C. It is discussed that for low-temperature growth of SWNTs, the plasma power should be held at a low level to avoid the formation of disordered or amorphous carbons. The low-temperature growth of SWNTs may enable compatible integration of SWNTs with current complementary metal-oxide-silicon technology.

Introduction

Because of their one-dimensional structure and unique electrical and chemical properties, carbon nanotubes (CNTs) are academically and industrially exciting materials and may be the most promising candidate to realize molecular electronics.^{1,2}

Syntheses of carbon nanotube powders have been achieved by several methods such as arc discharge, laser ablation, and HiPCo processes.^{3–5} Recently, a sonochemical route to single-walled carbon nanotubes (SWNTs) was shown to lower the synthesis temperature down to room temperature.⁶ CNTs synthesized by these techniques should be subsequently purified and then located in the right position to fabricate CNT-based device elements. Therefore, controlled positioning of CNTs on a defined region has been regarded as a crucial step for device integration.⁷

On the other hand, CNTs grown by chemical vapor deposition (CVD) can be more easily integrated in devices than the synthesized nanotubes since nanotubes are directly and selectively grown on catalysts such as iron, cobalt, and nickel.⁸ Before CNT growth, the catalyst is prepatterned as films or nanoparticles on a defined region by various techniques such as lithographic lift-off, soft lithography,

offset printing, template methods, and direct lithography.^{8–12} Recently, we reported that catalytic nanoparticles can be prepatterned by a direct photolithographic method using a simple mixture of ferrocene and conventional photoresist as a catalytic photoresist (Cat-PR), which plays roles as both a catalyst and a photoresist for SWNT patterned growth.¹³

Despite the promise of nanotubes grown by CVD, the high growth temperature (>800 °C) of CNTs is a barrier for device fabrication. Since lower growth temperatures significantly enhance the compatibility of CNT growth with current complementary metal-oxide-silicon (CMOS) technology for CNT-based electronics, plasma enhanced chemical vapor deposition (PECVD) has been recently utilized to grow nanotubes at lower temperatures.^{14–17} Unfortunately, the grown nanotubes at lower temperatures by PECVD are generally multiwalled carbon nanotubes (MWNTs).^{14,15} Using the microwave plasma chemical vapor deposition method, MWNTs were grown at ~450 °C by Wilson and co-workers.¹⁵ To our knowledge, the lowest growth temperature for SWNTs is 550 °C, reported by Kato and co-workers. They used radio frequency magnetron PECVD to grow

* Corresponding author. E-mail: wanjun@samsung.com.

- (1) Ouyang, M.; Huang, J. L.; Lieber, C. M. *Acc. Chem. Res.* **2002**, *35*, 1018–1025.
- (2) Avouris, P. *Acc. Chem. Res.* **2002**, *35*, 1026–1034.
- (3) Journet, C.; Maser, W. K.; Bemier, P.; Loiseau, A.; Chapelle, M. L.; Lefrant, S.; Deniard, P.; Lee, R.; Fischer, J. E. *Nature* **1997**, *388*, 756–758.
- (4) Guo, T.; Nikolaev, P.; Thess, A.; Colbert, D. T.; Smalley, R. E. *Chem. Phys. Lett.* **1995**, *243*, 49–54.
- (5) Nikolaev, P.; Bronikowski, M. J.; Bradley, R. K.; Rohmund, F.; Colbert, D. T.; Smith, K. A.; Smalley, R. E. *Chem. Phys. Lett.* **1999**, *313*, 91–97.
- (6) Jeong, S. H.; Koh, J. H.; Park, J. B.; Park, W. *J. Am. Chem. Soc.* **2004**, *126*, 15982–15983.
- (7) Dai, H. *Acc. Chem. Res.* **2002**, *35*, 1035–1044.
- (8) Kong, J.; Soh, H. T.; Cassell, A. M.; Quate, C. F.; Dai, H. *Nature* **1998**, *395*, 878–881.

- (9) Cassell, A. M.; Franklin, N. R.; Tomblor, T. W.; Chan, E. M.; Han, J.; Dai, H. *J. Am. Chem. Soc.* **1999**, *121*, 7975–7976.
- (10) Choi, W. B.; Chung, D. S.; Kang, J. H.; Kim, H. Y.; Jin, Y. W.; Han, I. T.; Lee, Y. H.; Jung, J. E.; Lee, N. S.; Park, G. S.; Kim, J. M. *Appl. Phys. Lett.* **1999**, *75*, 3129–3131.
- (11) Bae, E. J.; Choi, W. B.; Jeong, K. S.; Chu, J. W.; Park, G. S.; Song, S.; Yoo, I. K. *Adv. Mater.* **2002**, *14*, 277–279.
- (12) Huang, S.; Dai, L.; Mau, A. M. H. *Adv. Mater.* **2002**, *14*, 1140–1143.
- (13) Min, Y. S.; Bae, E. J.; Park, J. B.; Park, W. *Chem. Mater.* **2005**, submitted.
- (14) Delzeit, L.; MaAninch, I.; Cruden, B. A.; Hash, D.; Chen, B.; Han, J.; Meyyappan, M. *J. Appl. Phys.* **2002**, *91*, 6027–6033.
- (15) Wilson, J. I. B.; Scheerbaum, N.; Karim, S.; Polwart, N.; John, P.; Fan, Y.; Fitzgerald, A. G. *Diamond Relat. Mater.* **2002**, *11*, 918–921.
- (16) Kato, T.; Jeong, G. H.; Hirata, T.; Hatakeyama, R.; Tohji, K.; Motomiya, K. *Chem. Phys. Lett.* **2003**, *381*, 422–426.
- (17) Li, Y.; Mann, D.; Rolandi, M.; Kim, W.; Ural, A.; Hung, S.; Javey, A.; Cao, J.; Wang, D.; Yenilmez, E.; Wang, Q.; Gibbons, J. F.; Nishi, Y.; Dai, H. *Nano Lett.* **2004**, *4*, 317–321.

SWNTs at 550 °C with zeolites as a supporting template for the Fe/Co catalyst.¹⁶ Dai's group demonstrated that SWNTs can be grown at 600 °C without any template.¹⁷

Here, we report that SWNTs can be grown at 400–450 °C without any template by remote PECVD. It is discussed that the key process parameter to enable the low-temperature growth is low plasma power, which should be held at a minimum. This low-temperature growth may enhance the compatibility of SWNTs with current CMOS processes.

Experimental Procedures

Two types of catalysts were used in this work. The first was prepared from a simple mixture of ferrocene (Aldrich, 98%) and conventional photoresist (AZ 5214E, Clariant Co.).¹³ Different amounts of ferrocene were dissolved in 10 mL of AZ 5214E to obtain various concentrations (0.01–0.3 M) of precursor solutions. The solution was spin-coated on SiO₂ (400 nm)/Si wafers (1 cm × 1 cm) and baked at 100 °C for 2 min. Before the growth of CNTs, the substrate was burned at 550 °C for 30 min with an oxygen flow of 500 sccm (1.5 Torr) to remove organic substances and deposit catalytic nanoparticles on the substrate. The second type of catalyst, which was used only for the results in Figure 9, was deposited with a methanol (15 mL) suspension of Fe(NO₃)₃·9H₂O (0.05 mmol), MoO₂(acac)₂ (acac = acetylacetonate; 0.015 mmol), and alumina nanoparticles (Degussa, 14 nm; 15 mg).¹⁸ The suspension was dropped on the SiO₂/Si substrates, and after solvent vaporization at room temperature, the substrate was heated at 170 °C for 5 min.

A homemade radio frequency (rf, 13.56 MHz) remote PECVD system was used for CNT growth (see Figure S1 in Supporting Information for the schematic diagram). A quartz tube with a 2 in. diameter was surrounded by a copper coil in a helical manner from the gas inlet to the sample holder, which was located at a distance of 17 cm from the end of the copper coil. A rf generator with a maximum power of 1 kW was used to obtain plasma powers of 15 to 450 W. Lower plasma power than 15 W could not be utilized for the growth since forward power was not stable due to high reflected power. Substrates were heated by halogen lamps, and the growth temperature was calibrated with a thermocouple-implanted quartz holder. The calibrated temperature was not influenced by the remote plasma ignition.

Catalyst-deposited substrates were placed on a quartz holder and then heated to the growth temperature for 300 s in an argon atmosphere (100 sccm). After an interval for the stabilization of substrate temperature, methane (60 sccm) was introduced with argon (15 sccm) in the quartz tube, and the subsequent plasma was ignited to grow CNTs. During the CNT growth (10 min), the working pressure was maintained at ~0.4 Torr. CNT growth was performed in the growth temperature range of 350–500 °C, and the plasma power was varied in the range of 15–440 W.

Scanning electron microscopy (SEM) with a Hitachi S4500 instrument at an operating voltage of 20 kV was used to obtain images of CNT-grown surfaces. High-resolution transmission electron microscopy (HRTEM) with a FEI TECNAI G2-ST instrument at an operating voltage of 200 kV was also carried out to analyze nanotubes. The specimens for TEM analysis were prepared by dissolving the nanotubes detached from the substrate in acetone. Raman spectroscopy was used to characterize SWNTs grown on SiO₂ using 633 nm (Renishaw 3000) laser excitation with spot sizes of ~1 μm.

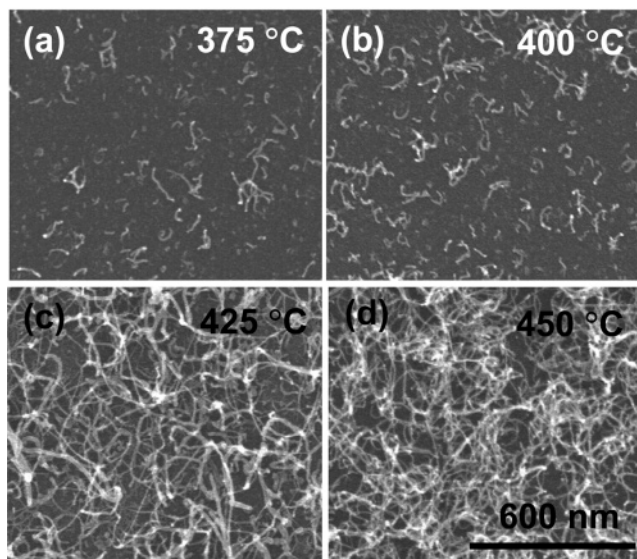


Figure 1. SEM images of nanotubes grown at 375 (a), 400 (b), 425 (c), and 450 °C (d) with a plasma power of 65 W using a 0.3 M catalytic solution.

Results and Discussion

Since the diameters of the nanotubes are determined by the diameters of the catalytic nanoparticles,^{19–21} we mainly used the mixture of ferrocene and AZ 5214E as a catalytic precursor solution, which gives nanoparticles with diameters of 3–10 nm.¹³ CVD was performed on SiO₂/Si substrates with catalytic nanoparticles in this work. For low-temperature growth of SWNTs, the plasma power and concentration of the catalyst solution were examined with growth temperature as process variables.

SEM images in Figure 1 show that the density of grown CNTs increases as the growth temperature increases. CNTs shown in Figure 1 were grown on catalytic nanoparticles obtained from a 0.3 M catalytic solution with a plasma power of 65 W. Nanotubes were not obtained below 350 °C but sparsely grown in the growth temperature range of 375–400 °C and densely grown above 425 °C. To evaluate the amount of disordered or amorphous carbons deposited during CNT growth, we monitored a Raman intensity ratio (I_D/I_G) of D- to G-band, as shown in Figure 4a. Since the G- and D-bands are due to tangential stretch modes of nanotubes and disordered graphite or amorphous carbons, respectively, the ratio generally increases with an increasing amount of disordered or amorphous carbons.²² At a temperature range of 375–425 °C, there is no significant variation in the ratio with the growth temperature. Merely, the ratio decreases from ~1.5 at 375–425 °C to ~1 at 450 °C, although the ratio is still high due to amorphous carbons being deposited with CNTs.

Concentration of the catalytic solution influences the density of nanotubes, as shown in Figure 2, which was

(18) Li, Y.; Kim, W.; Zhang, Y.; Rolandi, M.; Wang, D.; Dai, H. *J. Phys. Chem. B* **2001**, *105*, 11424.

(19) Kong, J.; Soh, H. T.; Cassell, A. M.; Quate, C. F.; Dai, H. *Nature* **1998**, *395*, 878.

(20) Cheung, C. L.; Kurtz, A.; Park, H.; Lieber, C. M. *J. Phys. Chem. B* **2002**, *106*, 2429.

(21) Han, S.; Yu, T.; Park, J.; Koo, B.; Joo, J.; Hyeon, T.; Hong, S.; Im, J. *J. Phys. Chem. B* **2004**, *108*, 8091.

(22) Dresselhaus, M. S.; Dresselhaus, G.; Jorio, A.; Souza Filho, A. G.; Saito, R. *Carbon* **2002**, *40*, 2043–2061.

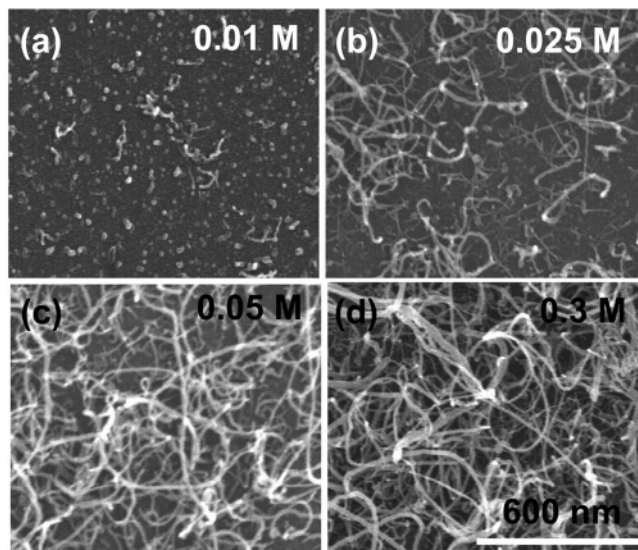


Figure 2. SEM images of nanotubes grown at 450 °C with a plasma power of 65 W using a 0.01 (a), 0.025 (b), 0.05 (c), and 0.3 M (d) catalytic solution.

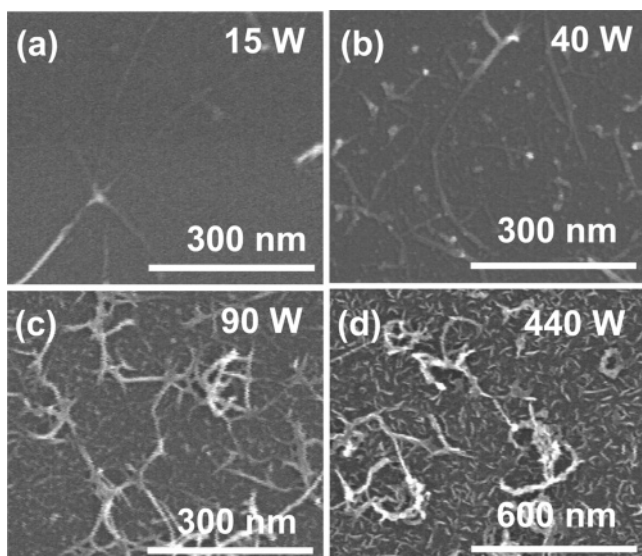


Figure 3. SEM images of nanotubes grown at 450 °C with plasma powers of 15 (a), 40 (b), 90 (c), and 440 W (d) using a 0.05 M catalytic solution.

performed at 450 °C with a plasma power of 65 W. The density of CNTs apparently increases as the concentration of catalytic solutions increases. However, the I_D/I_G ratio (Figure 4b) decreases as the concentration increases in concentrations below 0.05 M and then saturates at a value of around 1. Therefore, we chose the 0.05 M solution for further optimization.

To investigate the plasma power effect on nanotube growth, CNTs were grown at 450 °C with a catalytic solution of 0.05 M. In the low power region (<40 W, Figure 3a,b), CNTs are sparsely grown, but in the high power region, nanotubes with larger diameters are densely grown with short nanotubes or carbonaceous particles as shown in Figure 3c,d. The plasma effects are more clearly revealed in Figure 4c. The I_D/I_G ratio dramatically decreases from ~ 1.9 at 90 W to ~ 0.1 at 15 W as the plasma power decreases. However, the ratio is nearly constant in the high power region. It should be noted that the plasma lowers the growth temperature of nanotubes, but the power should be held at a minimum to avoid the increase of the I_D/I_G ratio.

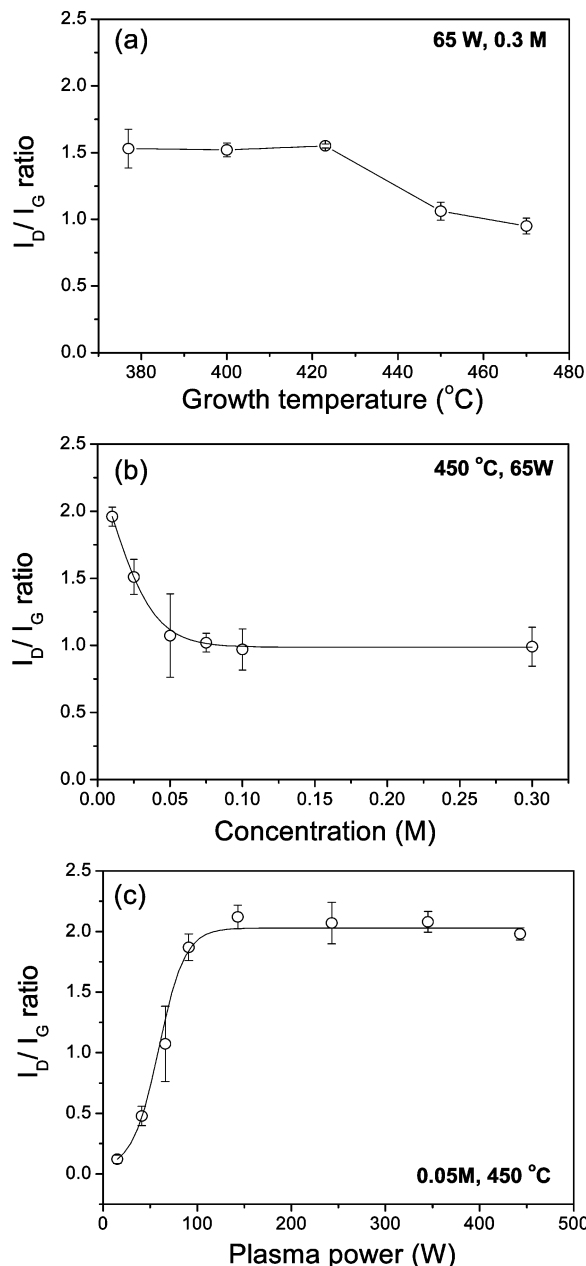


Figure 4. I_D/I_G ratio variations with growth temperature (a), concentration of catalytic solution (b), and plasma power (c).

Figure 5a shows G- and D-band peaks of CNTs prepared at a plasma power of 90, 40, and 15 W of which the I_D/I_G ratios were plotted in Figure 4c. Their corresponding radial breathing mode (RBM) peaks are shown in Figure 5b. The RBM peaks were not observed from CNTs grown with high power (>90 W) but mainly appear in the frequency range of 180–240 cm^{-1} from those grown with low power (15 and 40 W). Since SWNTs show characteristic RBM peaks with A_{1g} symmetry, it is proven that nanotubes grown with low power are mainly SWNTs or bundles. According to the diameter (d_t , nm)–frequency (ω_{RBM} , cm^{-1}) relationship for bundles of SWNTs ($\omega_{\text{RBM}} = 234/d_t + 10$),²³ the RBM peaks are due to nanotubes with a diameter range of 1.02–1.38 nm.

The higher frequency component (ω_{G^+}) and the lower frequency component (ω_{G^-}) of the G-band (Figure 5a) are

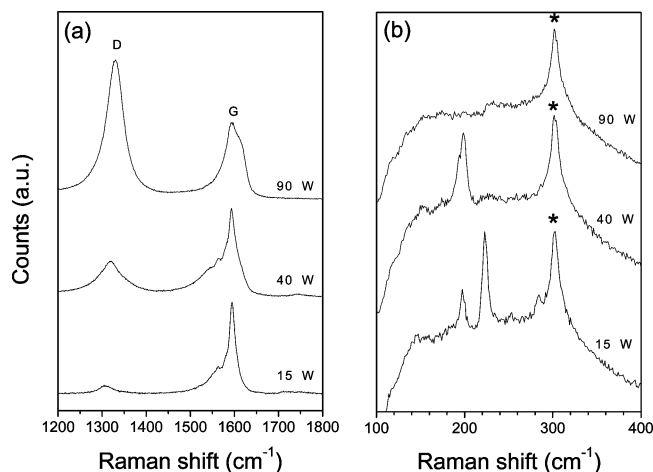


Figure 5. Raman spectra of nanotubes grown at 450 °C with plasma powers of 15, 40, and 90 W using a 0.05 M catalytic solution. (a) G- and D-bands. (b) Radial breathing modes. Raman spectra were obtained from 633 nm laser excitation at five different positions of each specimen and calibrated with a peak at 303 cm^{-1} due to the SiO_2/Si substrate, which is denoted with an asterisk.

attributed to vibrations along the direction of the nanotube axis and along the circumferential direction, respectively. The G band components, ω_{G}^+ and ω_{G}^- , are related with the equation $\omega_{\text{G}}^- = \omega_{\text{G}}^+ - c/d_t^2$ where $c = 47.7 \text{ cm}^{-1} \text{ nm}^2$ for semiconducting nanotubes and $c = 79.5 \text{ cm}^{-1} \text{ nm}^2$ for metallic nanotubes.²⁴ The sharp Lorentzian features of the peaks indicates that the grown SWNTs are mainly semiconducting.²² For metallic SWNTs, the lower frequency component generally shows a very broad Breit–Wigner–Fano line. It was recently reported that nearly 90% of the nanotubes grown at 600 °C by PECVD was semiconductors. For nanotubes grown at 15 W ($\omega_{\text{G}}^+ = 1595 \text{ cm}^{-1}$), substituting the diameter of 1.2 nm in the equation, the calculated value of ω_{G}^- for semiconducting nanotubes is 1562 cm^{-1} , which agrees well with the observed value (1564 cm^{-1}). This also supports that semiconducting nanotubes have a higher population than metallic nanotubes, although it is not clear if the semiconducting portion is higher than the ratio of semiconducting to metallic nanotubes (2:1) expected from random chirality distribution.

Figure 6 shows the $I_{\text{D}}/I_{\text{G}}$ ratio as a function of growth temperature for nanotubes grown from a 0.05 M catalytic solution with 15, 40, and 65 W plasma powers. The ratio was calculated with Raman spectra averaged from 5 to 15 different scans. Solid circles denote that RBM peaks were obtained from all of the scans. Process conditions showing RBM peaks from some scan positions were designated with open circles. Cross symbols represent no RBM peaks. Figure 6 clearly reveals that the plasma power should be low to obtain SWNTs showing RBM peaks with a low $I_{\text{D}}/I_{\text{G}}$ ratio at low temperatures. The lowest growth temperature showing RBM peaks from all of scans was 425 °C, but their $I_{\text{D}}/I_{\text{G}}$ ratios were higher than those of nanotubes grown at 450 °C. From the nanotubes grown at 400 °C with plasma powers of 15 and 40 W, the RBM peaks, respectively, appeared from three and two positions of five different scans. SWNT growth

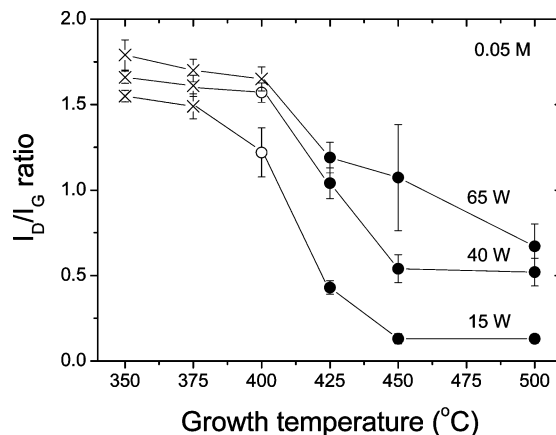


Figure 6. $I_{\text{D}}/I_{\text{G}}$ ratio variation with growth temperature. Solid or open circles designate that RBM peaks appear from all or a few of five different scans, respectively. Cross symbols indicate that RBM peaks were not observed from several scans.

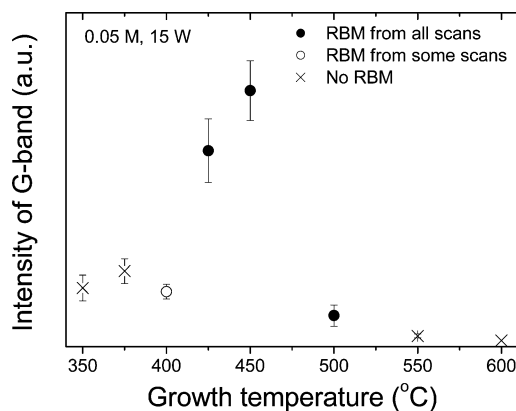


Figure 7. Intensity variation of G-band with growth temperature. The nanotubes were grown with a plasma power of 15 W using a 0.05 M catalytic solution.

may be suppressed by high plasma power due to the bombardment effect.²⁵ The importance of low plasma power is also supported by a previous report by Delzdit. In their work, MWNTs were grown at low power levels, and nanofibers were formed at high power levels, of which a transition occurred at 30–40 W.²⁶

Temperature effects on the intensity of the G-band were investigated with nanotubes grown from a 0.05 M catalytic solution using a low plasma power of 15 W. As the growth temperature increases, the intensity of the G-band shows an increasing tendency up to 450 °C and then decreases at higher temperatures than 450 °C as shown in Figure 7. Eventually, the G-band disappears at 600 °C, wherein any peak due to the carbon materials is not observed in Raman spectra. The disappearance of the Raman peaks may be attributed to an etch effect by plasma. To verify the etch effect by the weak plasma power, we treated nanotubes at 450 °C under argon plasma (15 W) without any flow of methane gas. As the plasma treatment time increased, the G-band was gradually weakened and nearly disappeared after 10 min (data not shown). Therefore, such a temperature dependency of the G-band in Figure 7 can be explained by a competition

(24) Jorio, A.; Souza Filho, A. G.; Dresselhaus, G.; Dresselhaus, M. S.; Swan, A. K.; Unlu, M. S.; Goldberg, B. B.; Pimenta, M. A.; Hafner, J. H.; Lieber, C. M.; Saito, R. *Phys. Rev. B* **2002**, *65*, 155412.

(25) Song, I. K.; Cho, Y. S.; Choi, G. S.; Park, J. B.; Kim, D. J. *Diamond Relat. Mater.* **2004**, *13*, 1210–1213.

(26) Delzeit, L.; McAninch, I.; Cruden, B. A.; Hash, D.; Chen, B.; Han, J.; Meyyappan, M. *J. Appl. Phys.* **2002**, *91*, 6027–6033.

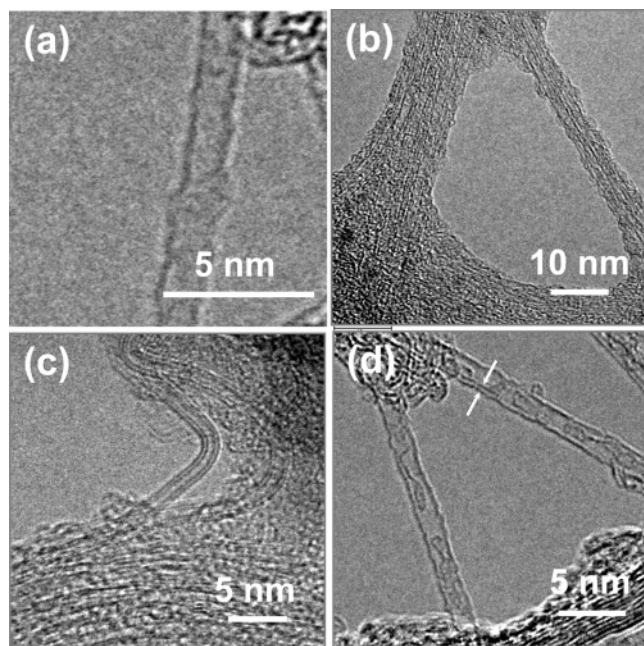


Figure 8. HRTEM images of nanotubes. (a) Single-walled nanotubes. (b) Bundles. (c) Double-walled nanotubes. (d) Single-walled nanotubes with carbonaceous materials inside. Nanotubes were grown at 450 °C with a plasma power of 40 W using a 0.05 M catalytic solution. Dark lines correspond to the sidewalls of nanotubes.

between growth and etch reactions of sp^2 carbon structures such as SWNTs, MWNTs, and graphene sheets. As the growth temperature increases, the contribution of the etch reaction may increase. When the etch effect is small, the G-band shows an increasing tendency with the temperature. However, as the etch effect increases, the G-band intensity gradually decreases with the growth temperature (>450 °C). At 600 °C, the growth of sp^2 carbons was eventually overcome by the etch effect, to result in the disappearance of the G-band. It should be noted that the RBM peaks with a strong G-band are obtained from the specimens grown at 425–450 °C, wherein the etch effect of sp^2 carbons is considerably high. This means that the etch effect by the low plasma power plays a critical role for SWNT growth.

The structure and diameter of SWNTs were confirmed with HR-TEM (see Figure S2 for a low magnification image of TEM). As a SWNT with a diameter of 1.2 nm is shown in Figure 8a, the diameters of the observed SWNTs agree well with the diameter range of 1.02–1.38 nm expected from the RBM peak positions. However, the observed nanotubes detached from the substrates for TEM analysis are mainly bundles, as shown in Figure 8b. Double-walled carbon nanotubes (DWNTs) were also observed with SWNTs. Figure 8c shows a DWNT with an outer diameter of 1.33 nm and an inner diameter of 0.61 nm. The interlayer distance of the DWNTs is ~ 0.36 nm, which is similar to reported values.²⁷ Figure 8d shows an image of SWNTs with carbonaceous materials. Interestingly, some of the carbonaceous materials form a partial double wall with the wall of nanotube. Furthermore, the interlayer distance is ~ 0.35 nm, which is nearly the same with that of Figure 8c. It is believed that such peapod-like structures are strongly related to the

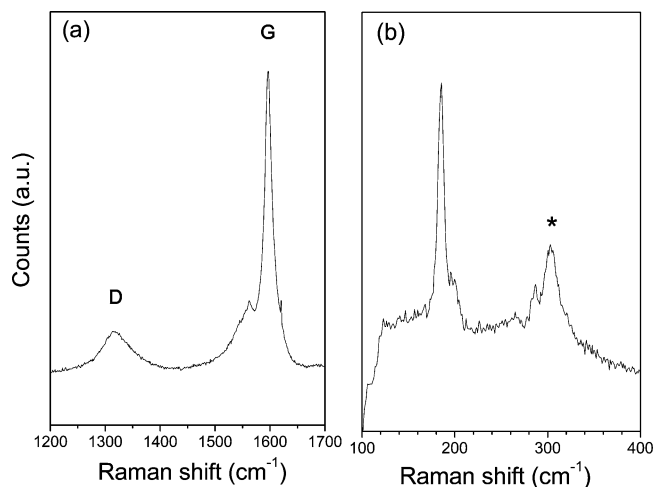


Figure 9. Raman spectra of nanotubes grown at 450 °C with a plasma power of 15 W using a methanol suspension of $Fe(NO_3)_3 \cdot 9H_2O$, $MoO_2(acac)_2$, and alumina nanoparticles. (a) G- and D-bands. (b) Radial breathing modes. Raman spectra were obtained from 633 nm laser excitation and calibrated with a peak at 303 cm^{-1} due to the SiO_2/Si substrate, which is denoted with an asterisk.

growth of DWNTs.²⁸ Recently, Hiraoka et al. suggested that an outer tube should be a template for the inner tube formation from observations of the peapod-like structures.²⁹

The remote-PECVD was carried out on a Fe/Mo catalyst with an alumina supporter reported by Dai et al.¹⁹ at 450 °C with a plasma power of 15 W. Raman spectra (Figure 9) from the specimen also show RBM peaks and a strong G-band, which are similar to the spectra shown in Figure 5. The presence of the RBM peaks in Figure 9 reveals that the successful growth of SWNTs by remote PECVD is not due to the special catalyst obtained from the catalytic solution, but the SWNT growth by using a low plasma power can be also utilized on other catalyst systems.

Conclusion

SWNTs with a small ratio ($I_D/I_G \sim 0.1$) of the D- to G-band were successfully grown at 450 °C by remote PECVD with a plasma power of 15 W. Even at 400 °C, SWNTs were also grown with low plasma powers (<40 W), although the I_D/I_G ratios are higher than those grown at 450 °C. To lower the growth temperature, the plasma power should be held at a minimum to avoid formation of disordered or amorphous carbons. The low-temperature growth of SWNTs may enable compatible integration of SWNTs with current CMOS technology.

Acknowledgment. This work was financially supported by the Tera-Level Nano-Devices (TND) Program of the Ministry of Science and Technology, Korea.

Supporting Information Available: Schematic diagram of remote-PECVD system and a low magnification TEM image of the grown nanotubes. This material is available free of charge via the Internet at <http://pubs.acs.org>.

CM050889O

(27) Wei, J.; Jiang, B.; Zhang, X.; Zhu, H.; Wu, D. *Chem. Phys. Lett.* **2003**, *376*, 753–757.

(28) Bandow, S.; Takizawa, M.; Hirahara, K.; Yudasaka, M.; Iijima, S. *Chem. Phys. Lett.* **2001**, *337*, 48–54.

(29) Hiraoka, T.; Kawakubo, T.; Kimura, J.; Taniguchi, R.; Okamoto, A.; Okazaki, T.; Sugai, T.; Ozeki, Y.; Yoshikawa, M.; Shinohara, H. *Chem. Phys. Lett.* **2003**, *382*, 679–685.